Interacting Targets of the Farnesyl of Transducin γ-Subunit[†]

Maiko Katadae,[‡] Ken'ichi Hagiwara,[‡,§] Akimori Wada,[||] Masayoshi Ito,[||] Masato Umeda,[⊥] Patrick J. Casey,[#] and Yoshitaka Fukada*[,‡]

Department of Biophysics and Biochemistry, Graduate School of Science, The University of Tokyo, Hongo, Bunkyo-ku, Tokyo 113-0033, Japan, Department of Organic Chemistry for Life Science, Kobe Pharmaceutical University, Higashinada-ku, Kobe, Hyogo 658-8558, Japan, Division of Supramolecular Biology, Institute for Chemical Science, Kyoto University, Gokasho, Uji, Kyoto 611-0011, Japan, and Department of Pharmacology and Cancer Biology, Duke University Medical Center, Durham, North Carolina 27710

Received March 1, 2008; Revised Manuscript Received May 19, 2008

ABSTRACT: G protein γ-subunits are isoprenylated and carboxyl methylated at the C-terminal cysteine residue, and the set of the posttranslational modifications is indispensable for the function of the photoreceptor G protein transducin (Tα/T$\beta\gamma$). To explore farnesyl-mediated molecular interactions, we investigated molecular targets of a T$\beta\gamma$ analogue that was engineered to have a photoreactive farnesyl analogue, (3-azidophenoxy)geranyl (POG), covalently bound to the C-terminal cysteine of Tγ. POG-modified T$\beta\gamma$ was further subjected to modification by methylation at the C-terminal carboxyl group, which copies a complete set of the known posttranscriptional modifications of T$\beta\gamma$. Photoaffinity labeling experiment with the photoreactive T$\beta\gamma$ analogue in its free form indicated that the POG moiety of Tγ interacted with Tβ. In the trimeric Tα/T$\beta\gamma$ complex, the POG moiety was cross-linked with Tα in addition to concurrent affinity labeling of Tβ. When photoreactive T$\beta\gamma$ was reconstituted with Tα and light-activated rhodopsin (Rh*) in rod outer segment (ROS) membranes, the POG moiety interacted with not only Tα and Tβ but also Rh* and membrane phospholipids. The cross-linked phospholipid species was analyzed by ELISA employing a variety of lipid-binding probes, which revealed phosphatidylethanolamine (PE) and phosphatidylserine (PS) as selective phospholipids for POG interaction in the ROS membranes. These results demonstrate that the modifying group of Tγ plays an active role in protein−protein and protein−membrane interactions and suggest that the farnesyl−PE/PS interaction may support the efficient formation of the signaling ternary complex between transducin and Rh*.

In vertebrate retinal rod outer segment (ROS),[1] light signals are transduced by the photoreceptor-specific G protein transducin, which links photolysis of rhodopsin to activation of cGMP-phosphodiesterase (PDE) (*1*). Transducin (Tα/T$\beta\gamma$) is comprised of three subunits: Tα (M_r 37000), Tβ (M_r 35000), and Tγ (M_r 8000). Tα contains a binding site for guanine nucleotide (GDP or GTP), whereas Tβ and Tγ form a tight complex (T$\beta\gamma$) which associates with Tα in its GDP-bound form (Tα-GDP). In phototransduction, Tα-GDP/T$\beta\gamma$ forms a transient ternary complex with a photobleached active intermediate of rhodopsin, metarhodopsin II (abbreviated as Rh* in this paper). Rh* facilitates exchange of GDP bound to Tα with cytosolic GTP, resulting in dissociation of the ternary complex into Tα-GTP, T$\beta\gamma$, and Rh*. A single molecule of Rh* catalyzes formation of several hundreds of Tα-GTP. The highly amplified element, Tα-GTP, in turn induces a release of the inhibitory γ-subunit from the catalytic core $\alpha\beta$ dimer of PDE, resulting in its activation. The activated PDE hydrolyzes cGMP, which causes hyperpolarization of the membrane potential via an impact on cGMP-dependent cation channels in rod cells. Thus, Rh*-transducin coupling achieves remarkable amplification of the photon signal in retinal rod photoreceptor cells (*1*).

We and others have reported that Tγ is farnesylated at its C-terminal cysteine residue via a thioether bond and, in addition, the C-terminal carboxyl group is methylated (*2, 3*). Subsequent cDNA cloning studies demonstrated that the deduced amino acid sequences of all 12 known subtypes of G protein γ-subunits share a common C-terminal CAAX motif (*4*). It is now established that posttranslational isoprenylation of the CAAX sequence proceeds via three enzymatic steps, isoprenylation at the cysteine residue in the CAAX motif, AAX cleavage, and then carboxyl methylation. The C-terminal amino acid X is a major determinant for the

[†] This work was supported in part by Grants-in-Aid from the Ministry of Education, Culture, Sports, Science and Technology, the Japanese Government, by a research grant from the Human Frontier Science Program to Y.F., and by NIH Grant GM46372 to P.J.C.

* Corresponding author. Telephone: +81 3 5841 4381. Fax: +81 3 5802 8871. E-mail: sfukada@mail.ecc.u-tokyo.ac.jp.

[‡] The University of Tokyo.

[§] Present address: Department of Biochemistry and Cell Biology, National Institute of Infectious Diseases, Shinjuku-ku, Tokyo, Japan.

[||] Kobe Pharmaceutical University.

[⊥] Kyoto University.

[#] Duke University Medical Center.

[1] Abbreviations: Tα, Tβ, and Tγ, the α-, β-, and γ-subunit of transducin, respectively; Rh*, metarhodopsin II; FTase, farnesyltransferase; ROS, rod outer segment; POG-PP, (3-azidophenoxy)geranyl pyrophosphate; Rce1, Ras converting enzyme 1; Icmt, isoprenyl carboxyl methyltransferase; AdoMet, *S*-adenosylmethionine; PE, phosphatidylethanolamine; PS, phosphatidylserine; PC, phosphatidylcholine; PIP_2, phosphatidylinositol 4,5-bisphosphate; SM, sphingomyelin; CBB, Coomassie Brilliant Blue R-250; PMSF, phenylmethanesulfonyl fluoride; β-ME, β-mercaptoethanol; ELISA, enzyme-linked immunosorbent assay.

10.1021/bi800359h CCC: $40.75
Published on Web 07/18/2008

modification by isoprenyl groups at the cysteine residue in the CAAX motif by either of the two cytosolic enzymes: protein farnesyltransferase (FTase) or protein geranylgeranyltransferase I (GGTase I) (*4*). Farnesylation (C15) by FTase occurs when X is serine, methionine, glutamine, or alanine, while the C-terminus is geranylgeranylated (C20) by GGTase I when X is leucine or phenylalanine (*5*). After isoprenylation, the AAX sequence in the CAAX motif is removed by a site-specific endoprotease, Ras converting enzyme 1 (Rce1) (*6*), and the prenylated cysteine residue newly exposed at the C-terminus is carboxyl methylated by a specific methyltransferase, isoprenylcysteine carboxyl methyltransferase (Icmt) (*7, 8*). Rce1 and Icmt have been shown to be microsomal membrane-bound enzymes (*6, 7*), and hence the processing of the prenylated CAAX motifs likely occurs on the microsomal membrane surface prior to the sorting of the fully processed prenylated proteins to the plasma membranes. Isoprenylation and the subsequent carboxyl methylation each confer hydrophobic property to the proteins, and therefore the modifications are generally regarded to enhance the membrane association of the protein. In fact, G$\beta\gamma$ or Ras proteins lacking CAAX motifs are unable to localize to plasma membranes (*9, 10*). On the other hand, several lines of evidence have suggested that the farnesyl and geranylgeranyl groups of transducin (*2, 4, 11–13*), Ras (*14*), and rhodopsin kinase (*15*) play key roles in protein−protein interactions. For example, mutant T$\beta\gamma$ consisting of Tγ truncated at the C-terminus, or T$\beta\gamma$ lacking the farnesyl moiety, is defective in catalyzing the GDP−GTP exchange reaction on Tα in the presence of Rh* (*2, 11, 12*). It has also been shown that synthetic peptides corresponding to the C-terminal region of Tγ inhibited Tα−T$\beta\gamma$ interaction only when the peptides were isoprenylated (*13*). T$\beta\gamma$ has another binding partner, phosducin (*16*), that is a soluble 33 kDa protein abundantly present in the inner region of the rod photoreceptor cells. Although phosducin is phosphorylated in the dark, it is dephosphorylated upon receiving intense light and binds to T$\beta\gamma$, which then loses its membrane-binding affinity (*16, 17*). The physiological roles of phosducin and its light-dependent dephosphorylation are still elusive, but one of its possible roles could be to inhibit T$\beta\gamma$ from interacting with Tα or effectors (*18*). The sequestration of T$\beta\gamma$ by phosducin may serve as a regulatory mechanism of the light signaling (*17–19*).

In addition to the farnesylation, the carboxyl methylation also plays a physiological role for isoprenylated proteins (*20*), such as T$\beta\gamma$ (*11, 12, 21*) and Ras (*10*). Our previous experiments showed that farnesylated and methylated T$\beta\gamma$ supported more efficiently the GDP−GTP exchange reaction on Tα catalyzed by Rh* when compared with farnesylated and nonmethylated T$\beta\gamma$ (*11, 12*). More evidently, the binding of farnesylated T$\beta\gamma$ to the ROS membranes was strongly facilitated by the carboxyl methylation (*12*). Together, these data indicate that the farnesylation of Tγ is indispensable for transducin to couple with Rh*, and the carboxyl methylation synergistically enhances this coupling. In spite of such an important role(s) of the farnesyl group, the interacting target(s) of the modifying lipid has not yet been directly demonstrated at each step of the signaling process. In structural studies on G proteins, the exact location of the isoprenoid group has not been identified by X-ray crystallography because most of the studies have employed engineered proteins lacking the prenyl group (*22, 23*).

In order to investigate farnesyl-mediated molecular interactions, several groups have synthesized photoreactive farnesyl analogues, among which (2-diazo-3,3,3-trifluoropropionyloxy)geranyl pyrophosphate (abbreviated as DATFP-GPP) was successfully recognized by prenyltransferase (*24, 25*). The interaction between the prenyltransferase and DATFP during the transfer reaction has been demonstrated, but possibly due to the chemical instability of DATFP, only a few labeling experiments have been performed successfully with the photoreactive compound incorporated into G protein after the transfer reaction. A single paper reported photoaffinity labeling of GDI with DATFP-modified Rab5 (*26*). On the other hand, we previously developed another photoreactive farnesyl analogue, (3-azidophenoxy)geranyl pyrophosphate (abbreviated as POG-PP), which has the photoreactive azidophenoxy group at the distal end of the structure, and created *in vitro* a functional (but nonmethylated) T$\beta\gamma$ analogue in which the farnesyl was replaced by POG (*27*). In the present study, we have generated the carboxyl methylated POG-T$\beta\gamma$ (POG-T$\beta\gamma$-OMe) by utilizing the processing enzymes, FTase, Rce1, and Icmt, in order to examine the mode of molecular interaction of the POG moiety in the T$\beta\gamma$ analogue having the complete set of modifications at the C-terminus of Tγ.

EXPERIMENTAL PROCEDURES

Materials. [^{35}S]GTPγS was purchased from NEN DuPont. Phospholipase A_2 (PLA_2, *Apis mellifera*), sphingomyelinase (SMase, *Bacillus cereus*), phosphatidylcholine (PC, derived from bovine brain), phosphatidylethanolamine (PE, derived from bovine brain), phosphatidylserine (PS, derived from bovine brain), phosphatidylinositol 4,5-bisphosphate (PIP_2, derived from bovine brain), sphingomyelin (SM, derived from bovine brain), *S*-adenosylmethionine (AdoMet), and cytochrome *c* were purchased from Sigma. Anti-Tα (sc-389), anti-Gβ (sc-261), and anti-Tγ (sc-373) antibodies were purchased from Santa Cruz Biotechnology, Inc. Anti-PC antibody (JE-1), anti-PIP_2 antibody (AM212), anti-lysenin antibody, and lysenin were established as described (*28–30*). Biotinylated Ro09-0198 (*31*) was a kind gift from Roche, Ltd. (Japan). Anti-PS antibody (1H6) was purchased from Upstate Group, Inc. Frozen bovine retina was purchased from WL Lawson Co.

Buffers. Buffer C, 20 mM Tris-HCl (pH 7.4 at 25 °C), 2.5 mM LiCl, 5 mM KCl, 1 mM β-ME, and 0.1 mM PMSF; buffer D, 20 mM Tris-HCl (pH 7.4 at 25 °C), 2 mM $MgCl_2$, 1 mM β-ME, 0.1 mM PMSF, 4 μg/mL aprotinin, and 4 μg/mL leupeptin; buffer P, 20 mM Tris-HCl (pH 7.6 at 25 °C), 2 mM $MgCl_2$, 5 μM $ZnCl_2$, 25 μM $MnCl_2$, and 1 mM β-ME; buffer R, 10 mM MOPS−NaOH (pH 7.5 at 4 °C), 30 mM NaCl, 60 mM KCl, 2 mM $MgCl_2$, 1 mM β-ME, 0.1 mM PMSF, 4 μg/mL aprotinin, and 4 μg/mL leupeptin; buffer W, 100 mM Tris-HCl (pH 7.5 at 4 °C) and 1 mM $MgCl_2$; TBS, 50 mM Tris-HCl (pH 7.4 at 25 °C), 200 mM NaCl, and 1 mM $MgCl_2$.

Preparation of POG-T$\beta\gamma$-OMe. The unmodified form of T$\beta\gamma$ (designated T$\beta\gamma$-VIS, containing Tγ with the nascent C-terminal sequence of Cys^{71}-Val^{72}-Ile^{73}-Ser^{74}) was expressed in *Trichoplusia ni* (Tn5) insect cells using a baculovirus

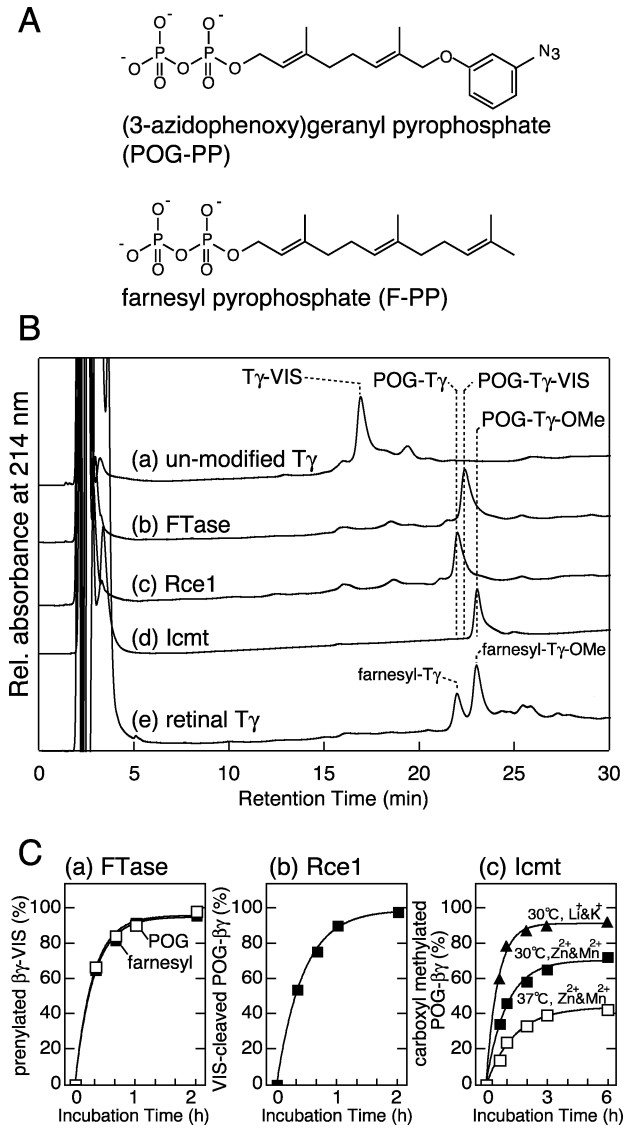

FIGURE 1: (A) Structures of POG-PP [(3-azidophenoxy)geranyl pyrophosphate] and farnesyl pyrophosphate. (B) HPLC analysis of Tγ in each modification step. Unmodified T$\beta\gamma$-VIS was incubated with yeast FTase in the presence of POG-PP, and aliquots of the reaction mixtures were subjected to reverse-phase HPLC analysis before (trace a) and after (trace b) the POG-transfer reaction. The analysis was also performed following Rce1 treatment (trace c) and Icmt treatment in the presence of AdoMet (trace d). Retinal Tγ was analyzed as a standard (trace e). HPLC analysis was performed as described in Experimental Procedures. Each peak fraction detected by the absorbance at 214 nm was collected and analyzed by MALDI-TOF mass spectrometry with the Voyager-DE (Applied Biosystems) spectrometer. The singly and doubly protonated ion signals of cytochrome *c* (from horse heart, M_r = 12359.7) were used as an internal standard of mass calibration. The observed $[M + H]^+$ values of the peak fractions were 8411.0 (trace a), 8681.1 (trace b), 8381.6 (trace c), and 8395.4 (trace d), in good agreement with the calculated $[M + H]^+$ values of Tγ-VIS (8411.4), POG-Tγ-VIS (8680.8), POG-Tγ (8381.4), and POG-Tγ-OMe (8395.4), respectively. Due to adsorption, Tβ was not eluted from the column. (C) Time courses of prenyl transfer (panel a), VIS cleavage (panel b), and carboxyl methylation (panel c) reactions catalyzed by FTase, Rce1, and Icmt, respectively.

expression system and purified as described previously (*4*). Recombinant yeast FTase was purified from a soluble fraction of the *Escherichia coli* cell lysate according to the method described previously (*27*). POG-PP (Figure 1A) was synthesized from geraniol as described (*27*). For the transfer reaction of POG-PP to T$\beta\gamma$, a mixture of unmodified T$\beta\gamma$-VIS (1 μM, final concentration) and 10 μg of FTase was prewarmed at 37 °C and then mixed with 100 μM final concentration of POG-PP in buffer P, adjusting the total volume to 10 mL with buffer P. The transfer reaction was carried out at 37 °C for 2 h. To monitor the transfer yield of the POG moiety to Cys^{71} of Tγ-VIS, aliquots of the reaction mixture were subjected to a reverse-phase HPLC system (model 600E; Waters) equipped with a Develosil 300 C4-HG-5 column (4.6 × 150 mm; Nomura Chemical, Kyoto, Japan); the elution was carried out with a linear gradient of acetonitorile (30−60%, 0.5%/min) in 0.05% trifluoroacetic acid at a flow rate of 1.0 mL/min. The eluate was monitored by absorbance at 214 nm (*4*), and the peak fractions were collected and subjected to mass spectrometric analysis using a Voyager-DE MALDI-TOF spectrometer (Applied Biosystems, Foster City, CA) for verification of the obtained products. In the HPLC analysis (Figure 1B), Tγ-VIS gave a peak with a retention time of 17.85 min (trace a). When the POG-transfer reaction proceeded, the peak corresponding to Tγ-VIS became small, and a new peak with a longer retention time of 24.05 min (trace b) was detected, indicating that Tγ-VIS was converted to a more hydrophobic species, POG-Tγ-VIS. In MALDI-TOF mass spectrometric analysis, the new peak fraction provided a *m/z* value of 8681.1 ($M + H^+$), which was in a good agreement with the calculated *m/z* value of POG-Tγ-VIS (*m/z* = 8680.6).

POG-T$\beta\gamma$-VIS thus obtained was then digested with recombinant Rce1 to cleave off the tripeptide VIS (-Val^{72}-Ile^{73}-Ser^{74}). For this, recombinant baculovirus encoding yeast Rce1 cDNA was infected to *Spodoptera frugiperda* (Sf9) insect cells to express recombinant Rce1, and 200 μg of the Sf9 membranes was added to POG-T$\beta\gamma$-VIS in 10 mL reaction mixture in buffer P. The proteolytic reaction was conducted at 37 °C for 2 h. To assess the completion of the cleavage reaction, aliquots of the reaction mixture were centrifuged at 20000*g* at 4 °C for 20 min to remove the Sf9 membranes, and the supernatants were injected onto the reverse-phase HPLC system as described above. A peak corresponding to POG-Tγ-VIS with a retention time of 24.05 min (Figure 1B, trace b) completely shifted to a new peak with shorter retention time of 23.75 min (trace c). In MALDI-TOF mass spectrometric analysis, this new peak fraction gave a *m/z* value of 8381.6 ($M + H^+$), which was in good agreement with the calculated *m/z* of POG-Tγ (*m/z* = 8381.4).

Because the FTase activity increases with Zn^{2+} and Mn^{2+} ions (*32*), we carried out the POG-transfer reaction and the subsequent VIS-cleavage reaction in the presence of 5 μM $ZnCl_2$ and 25 μM $MnCl_2$ (buffer P). These divalent ions, however, display an inhibitory effect toward Icmt, while monovalent cations such as Li^+ and K^+ exhibit stimulatory effect on Icmt (*33*). Therefore, prior to the next methylation step, we changed the buffer (i.e., Zn^{2+} and Mn^{2+} were replaced by Li^+ and K^+) by subjecting POG-T$\beta\gamma$ to MonoQ column chromatography in the presence of 2.5 mM LiCl and 5 mM KCl (buffer C). Briefly, the reaction mixture (after the cleavage reaction) containing fully POG-modified and VIS-cleaved T$\beta\gamma$ (designated POG-T$\beta\gamma$) was centrifuged at 20000*g* at 4 °C for 20 min to remove the membraneous debris, and the supernatant was subjeced to MonoQ column (HR50/5, Pharmacia) chromatography with a linear gradient

of NaCl (0−500 mM, 8.3 mM/min) in buffer C using a fast protein liquid chromatography (FPLC) system (Amersham Pharmacia) at a flow rate of 0.5 mL/min.

POG-T$\beta\gamma$ was then carboxyl methylated by incubation with Icmt and *S*-adenosylmethionine (AdoMet). Sf9 insect cells were infected with recombinant baculovirus encoding yeast Icmt cDNA to express recombinant Icmt, and 400 μg of the Sf9 membranes and 10 μM final concentration of AdoMet were added to POG-T$\beta\gamma$ in the 10 mL reaction mixture in buffer C. The carboxyl methylation reaction was conducted at 30 °C for 3 h. To assess the completion of carboxyl methylation, aliquots of the reaction mixture were centrifuged at 20000*g* at 4 °C for 20 min to remove the Sf9 membranes, and the supernatants were injected onto the reverse-phase HPLC system. A peak containing POG-Tγ with a retention time of 23.75 min (Figure 1B, trace c) shifted to a new peak with a longer retention time of 24.75 min (trace d). In MALDI-TOF mass spectrometric analysis, the eluate in this new peak fraction gave a *m*/*z* value of 8395.4 ($M + H^+$), which was in good agreement with the calculated *m*/*z* value (*m*/*z* = 8395.4) of carboxyl methylated POG-Tγ (designated POG-Tγ-OMe).

For purification of the final product, the reaction mixture was centrifuged at 20000*g* at 4 °C for 20 min to remove the membranous debris of Sf9. The supernatant was subjected to MonoQ column (HR5/5) chromatography using the FPLC system (Amersham Pharmacia). The proteins absorbed to the column were washed with buffer D and eluted with a linear gradient of NaCl (0−500 mM, 8.3 mM/min) formed in buffer D at a flow rate of 0.5 mL/min. Thus POG-T$\beta\gamma$-OMe was purified.

Preparation of Retinal Transducin and Phosducin. Transducin subunits, Tα and T$\beta\gamma$, were purified from bovine retinas as described previously (*4, 12*). The purified T$\beta\gamma$ fraction contained two subspecies of farnesylated T$\beta\gamma$ complex, each having either methylated or nonmethylated Tγ, and these subspecies were further separated by Superdex 75 prep grade column (HiLoad 26/60; Pharmacia) chromatography. The farnesylated and carboxyl methylated form of retinal T$\beta\gamma$ was used in this study. Recombinant rat phosducin was expressed in *E. coli* and purified as described previously (*27*).

Preparation of Transducin-Depleted Rod Outer Segment Membranes. ROS membranes were prepared from dark-adapted bovine retinas (*12*). Transducin-depleted ROS membranes were prepared in the dark by washing the ROS membranes seven times with buffer R containing 100 μM GTP and then washed three times with the same buffer containing 10 μM GTPγS. Finally, the ROS membranes were washed five times with the buffer R. Rhodopsin concentration was determined spectrophotometrically (*12*). Opsin membranes, in which rhodopsin was converted to inactive opsin plus retinal oxime, were prepared as described previously (*12*).

GTPγS-Binding Assay. To assess GTPγS binding by transducin, the dark-adapted and transducin-depleted ROS membranes were irradiated with an orange light (>540 nm) at 4 °C for 4 min to convert rhodopsin to Rh*. The binding assay was initiated by the addition of [^{35}S]GTPγS (370 GBq/mmol) to the mixtures containing various concentrations of Tα, T$\beta\gamma$, and Rh* (*4, 12*). The GTPγS-binding reactions were terminated at indicated times of the incubation by diluting 10 μL aliquots of the reaction mixture into 180 μL of ice-cold buffer W containing 2 mM GTP, and they were filtered through 0.45 μm cellulose membrane (type HATF; Millipore) fitted with MultiScreen Assay System (Millipore). The membranes were washed with 200 μL of buffer W in the MultiScreen Assay System assembly. The cellulose membranes were dissolved with 200 μL of 2-methoxyethanol, and the radioactivity was determined by liquid scintillation following addition of 800 μL of scintillation cocktail (ACS II; Amersham Biosciences).

Photoaffinity Labeling Experiments. Photoaffinity labeling experiments were performed in buffer D containing 0.2 mg/mL soybean trypsin inhibitor. The reaction mixtures (100 μL, final volume) containing the indicated combination of 0.2 μM POG-T$\beta\gamma$-OMe, 0.2 μM Tα, and 1.0 μM Rh* (or opsin with retinal-oxime) in the ROS membranes were incubated on ice for 30 min, after which they were placed at 4 cm distance from a 20 W suntan light with an illuminating spectrum peaking around 300 nm. Three cycles of irradiation (45 s each) were applied at 60 s intervals. After the UV irradiation, the samples containing the ROS membranes were centrifuged at 20000*g* at 4 °C for 20 min in order to separate the supernatant from the membrane fraction. The separated samples were subjected to SDS−PAGE for immunoblot analysis and for CBB staining. For better resolution of the cross-linked products in SDS−PAGE, the method of Laemmli's protocol (*34*) was modified by raising twice the concentration of Tris and glycine in the electrophoresis buffer and twice the concentration of Tris in the separation gel. Signals in the immunoblot were detected by CDP-Star chemiluminescent reagents (New England Biolabs) with the aid of Hyperfilm-ECL films (Amersham Pharmacia Biotech).

Extraction of Tγ−X from Rod Outer Segment Membranes. Samples (4 mL) containing 2.0 μM POG-T$\beta\gamma$-OMe, 2.0 μM Tα, and 10 μM Rh* were incubated at 4 °C for 30 min and then UV irradiated as described above. The sample after UV irradiation was centrifuged at 20000*g* at 4 °C for 20 min to recover the membrane fraction as a pellet. The pellet was washed three times with buffer R containing 10 μM GTPγS in order to remove Tα and non-cross-linked POG-T$\beta\gamma$-OMe. The final membrane pellet was mixed with recombinant phosducin (2.0 μM, final concentration), and the mixture was incubated at 4 °C for 10 min. After the mixture was centrifuged at 20000*g* at 4 °C for 20 min, the resultant pellet was homogenized with 1.0% CHAPS in buffer R. The homogenate was centrifuged at 20000*g* at 4 °C for 20 min, and the supernatant containing the cross-linked product of Tγ−X was subjected to the reverse-phase HPLC (model 600E; Waters) system equipped with the Develosil 300 C4-HG-5 column. Elution was carried out with a linear gradient of acetonitorile (30−80%, 1.0%/min) in 0.05% trifluoroacetic acid at a flow rate of 1.0 mL/min. The eluate was monitored by the absorbance at 214 nm, and 1 mL fractions were collected. A 10 μL aliquot of each fraction was subjected to SDS−PAGE followed by immunoblot analysis using anti-Tγ antibody, and the fractions containing Tγ−X were pooled for the ELISA analysis (see below). As a control, the ROS membranes with UV irradiation were homogenized with 1.0% CHAPS in buffer R in parallel. The homogenate was centrifuged at 20000*g* at 4 °C for 20 min, and the supernatant was applied to HPLC under the same condition. The fractions were collected at the same elution time as those of Tγ−X-containing fractions were pooled as a lipid background reference fraction (ROS control) for the ELISA analysis.

ELISA Analysis. Enzyme-linked immunosorbent assay (ELISA) was performed in 96-well microtiter plates (PolySorp; Nalgen Nunc) as described previously (*30*). Briefly, the pooled Tγ−X product (approximately 20 pmol) isolated by reversed-phase HPLC (see above) was adsorbed to the wells by incubating at 25 °C for 1.5 h. Similarly, retinal Tγ (20 pmol) was immobilized as a positive control for anti-Tγ detection. As a positive control for each lipid species, the wells were coated with 50 pmol (in 50 μL of ethanol) of either PE, PS, PC, PIP_2, or SM according to the methods previously described (*30*). As a negative control for the lipid background, the wells were coated with pooled HPLC fractions obtained from the UV-irradiated ROS membranes (ROS control; see above). The wells were blocked with 100 μL of 3.0% bovine serum albumin (BSA) in TBS at 25 °C for 2 h and then incubated at 25 °C for 2 h with 50 μL of anti-Tγ antibody, biotinylated Ro09-0198 (PE-binding peptide), anti-PS antibody (1H6), anti-PC antibody (JE-1), anti-PIP_2 antibody (AM212), or lysenin (SM-binding protein) all dissolved in 1.0% BSA/TBS. The wells incubated with lysenin were washed with 1.0% BSA/TBS to remove unbound lysenin and subsequently incubated with anti-lysenin antibody in 1.0% BSA/TBS at 25 °C for 2 h. The wells were then washed with 1.0% BSA/TBS and incubated with horseradish peroxidase-conjugated secondary probes (streptavidin for biotinylated Ro09-0198; anti-mouse IgG for anti-PS, -PC, and -PIP_2 antibodies; anti-rabbit IgG for anti-lysenin and Tγ antibodies) in 1.0% BSA/TBS 25 °C for 1 h. After the incubation, the wells were washed three times with TBS, and 100 μL of 3,3′,5,5′-tetramethylbenzidine solution (100 μg/mL) was added to the wells as a chromophore substrate. After incubation at 25 °C for 5 min, the reaction was quenched by the addition of 1 M H_2SO_4 (100 μL), and the absorbance at 492 nm (minus that at 600 nm for reference) was read on an MPR-A4 microphotometer (TOSOH, Tokyo, Japan).

RESULTS

Preparation of POG-T$\beta\gamma$-OMe and Assessment of Its Ability To Support Transducin Function. The transfer reaction of POG to Cys^{71} of unmodified Tγ (Tγ-VIS) in T$\beta\gamma$ complex was efficiently catalyzed by recombinant yeast FTase (*27*): Tγ-VIS was modified almost completely with POG (Figure 1B, traces a and b) by incubation with FTase at 37 °C for 1.5 h (Figure 1C, panel a). Cleavage of the C-terminal VIS sequence of POG-T$\beta\gamma$-VIS by treatment with Rce1 at 37 °C for 2 h yielded the maximal cleavage (Figure 1C, panel b). The newly exposed carboxyl group of the C-terminal POG-modified cysteine residue was then methylesterified by using recombinant yeast Icmt with AdoMet as a substrate. We found that the carboxyl methylation reached a plateau with its maximum yield within 3 h incubation at 30 °C when Zn^{2+}/Mn^{2+}-containing buffer (buffer P) was replaced by 2.5 mM LiCl/5 mM KCl-containing buffer C (Figure 1C, panel c). The final product of POG-modified, VIS-cleaved, and carboxyl methylated T$\beta\gamma$ (designated POG-T$\beta\gamma$-OMe) was purified by MonoQ column chromatography.

The function of POG-T$\beta\gamma$-OMe in promoting the binding of GTPγS to Tα in the presence of Rh* was compared with retinal T$\beta\gamma$ in the farnesylated and carboxyl methylated form. Rh*-catalyzed binding of GTPγS to Tα was not stimulated by unmodified T$\beta\gamma$-VIS (Figure 2B, closed triangles), whereas doubly modified POG-T$\beta\gamma$-OMe (open circles) exhibited T$\beta\gamma$ activity similar to or slightly lower than that of the completely modified form of retinal T$\beta\gamma$ (closed circles), indicating that the POG moiety can functionally substitute for the farnesyl that is indispensable for the Rh*-mediated transducin activation (Figure 2B, compare closed circles with triangles).

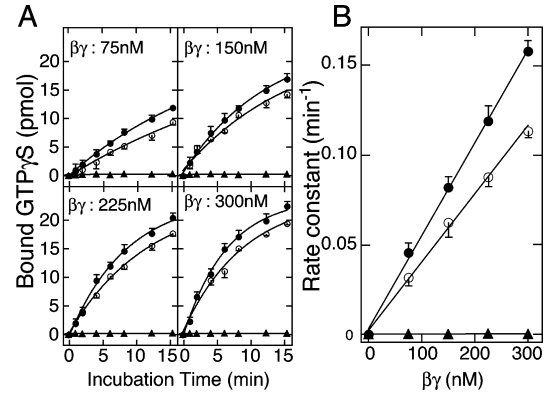

FIGURE 2: Rh*-catalyzed GTPγS binding to Tα stimulated by POG-T$\beta\gamma$-OMe. (A) Time courses of GTPγS binding to Tα in the presence of various concentrations of POG-T$\beta\gamma$-OMe (open circles), farnesyl-T$\beta\gamma$-OMe (closed circles), and unmodified T$\beta\gamma$-CVIS (closed triangles). Each reaction was carried out in a set of duplicate mixtures (each 100 μL) composed of various concentrations of POG-T$\beta\gamma$-OMe or farnesyl-T$\beta\gamma$-OMe (75, 150, 225, and 300 nM), 0.8 μM retinal Tα, 30 nM Rh* in ROS membranes, 0.002% Lubrol PX, 2.5 mg/mL ovalbumin, and 10 μM [^{35}S]GTPγS (74 MBq/mmol) in 10 mM MOPS−NaOH buffer (pH 7.5) containing 1 mM $MgCl_2$. The reaction was initiated by the addition of [^{35}S]GTPγS, and at the indicated times of incubation at 0 °C, 10 μL aliquots were transferred to MultiScreen filter cups (Millipore; 0.45 μm cellulose membrane) filled with 180 μL of 100 mM Tris-HCl (pH 7.5, at 0 °C) containing 1 mM $MgCl_2$ and 2 mM GTP to quench GTPγS binding. Filters were washed four times and the radioactivity was determined by a liquid scintillation method as described. The data were fitted to the equation $B(t) = B_{max}$ (1 − exp(−kt)), where $B(t)$ is the amount of bound GTPγS at time = t (min) and B_{max} (in pmol) is the maximum binding at infinite time. Each data point is the average ± variation of duplicate determinations from a single experiment, and a representative set of data from experiments repeated three times is shown. (B) The rate constants (k) calculated from (A) were plotted against the concentrations of POG-T$\beta\gamma$-OMe (open circles), farnesyl-T$\beta\gamma$-OMe (closed circles), and unmodified T$\beta\gamma$-VIS (closed triangles). Each data point is the average ± SD of three independent measurements of the time constant as exemplified in (A).

Photoaffinity Labeling Experiments of POG-T$\beta\gamma$-OMe. As an initial assessment of the binding interactions of POG-T$\beta\gamma$-OMe, we performed UV-stimulated affinity labeling experiments with doubly modified $\beta\gamma$ in solution in the presence or absence of Tα-GDP, and the UV-cross-linked product was immunoblotted with anti-Tγ antibody (Figure 3A, panel a). In the absence of Tα, anti-Tγ antibody detected a cross-linked product of 43 kDa (lane 3) in addition to free Tγ (8 kDa), whereas in the presence of equimolar Tα, an additional 45 kDa product was detected (lane 4). These 43/45 kDa products were not detected in UV-irradiated retinal T$\beta\gamma$ (lane 1) nor in the sample without UV irradiation (lane 2), indicating that the 43 and 45 kDa products were formed by the photoreaction dependent on POG and UV irradiation. The 43 kDa product was also immunoreactive to anti-Gβ antibody (Figure 3A, panel c), and therefore the 43 kDa band represented a cross-linked product of POG-Tγ-OMe (8 kDa)

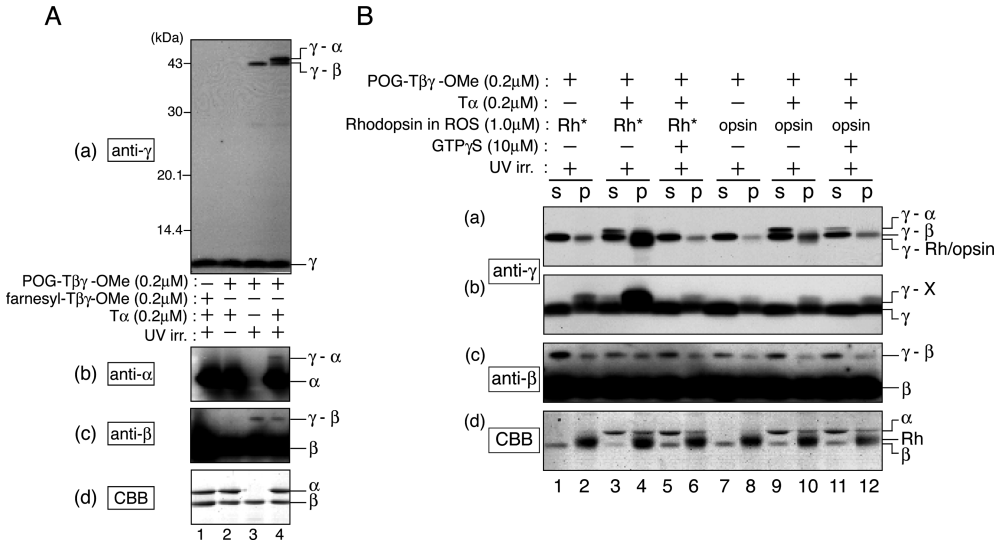

FIGURE 3: Photoaffinity labeling experiments in solution (A) and in ROS membranes (B). (A) Each sample (100 μL) contained the indicated combinations of 0.2 μM POG-Tβγ-OMe or retinal Tβγ (farnesyl-Tβγ-OMe) and 0.2 μM Tα (at final concentration). After UV irradiation, the samples were subjected to SDS−polyacrylamide gel (12.5%) electrophoresis. Proteins were transferred to a PVDF membrane for immunostaining by anti-Tγ (panel a), anti-Tα (panel b), or anti-Gβ (panel c) antibodies or CBB-stained (panel d). (B) Each sample (100 μL) contained the indicated combinations of 0.2 μM POG-Tβγ-OMe, 0.2 μM Tα, 1.0 μM Rh* or opsin in ROS membranes, and 10 μM GTPγS (at final concentration). After UV irradiation, the samples were centrifuged to obtain the supernatant (s) and the membrane pellet (p), which were subjected to SDS−polyacrylamide gel (12.5%) electrophoresis. Proteins were transferred to a PVDF membrane for immunostaining by anti-Tγ and anti-Gβ antibodies. Shown are the clipped images of the anti-Tγ blot at the 30−50 kDa region (panel a) or at the gel front region (panel b), anti-Gβ blot at 30−50 kDa (panel c), and the CBB-stained gel at the 30−50 kDa region (panel d). Shown is a representative set of data from experiments repeated five times with similar results.

and Tβ (35 kDa). On the other hand, the 45 kDa product was detected by anti-Tα antibody (panel b), and hence the 45 kDa product was assigned to a cross-linked product of POG-Tγ-OMe (8 kDa) and Tα (37 kDa).

To explore the role of the farnesyl moiety in the receptor/G protein coupling, we next studied the molecular interaction in the presence of Rh* in membranes, which was prepared by exposure of the transducin-depleted ROS membranes to an orange light (>540 nm) to convert rhodopsin to Rh* prior to cross-linking. After UV irradiation, the reaction mixtures were centrifuged to investigate the distribution of the cross-linked products in the supernatant (Figure 3B, lanes labeled by "s") and in the membrane (labeled by "p") fractions. UV irradiation of POG-Tβγ-OMe in the presence of Rh*-containing ROS membranes yielded the 43 kDa band of Tγ−Tβ cross-linked product, which was present in both the soluble and the membrane fractions (Figure 3B, panels a, lanes 1, 2). When Tα-GDP was added to the reaction mixture, the 45 kDa band of Tγ−Tα cross-linked product was detected in the supernatant (Figure 3B, panel a, lane 3). This cross-linked product disappeared when the mixture received 10 μM GTPγS (lane 5), showing that Tα-GDP conversion to the GTPγS-bound form results in the Rh*/Tα/Tβγ ternary complex decomposing into the three components. This observation therefore indicates a transient and stage-specific interaction between the modifying lipid of Tγ and Tα-GDP. On the other hand, no significant effect of Tα nor GTPγS was observed for Tγ−Tβ cross-link level in the membrane pellet (panel c, lanes 2, 4, and 6), suggesting a default position of the modifying lipid of Tγ in the Tβ pocket.

In the presence of Tα-GDP and Rh*-containing ROS membranes, a broad band of 43 kDa product was detected by anti-Tγ antibody in the membrane fraction (Figure 3B, panel a, lane 4). The 43 kDa broad band was not observed in our previous study using the nonmethylated form of POG-Tβγ under the equivalent experimental condition (*27*). The 43 kDa broad band was not attributable to Tγ−Tβ cross-linked product, because the anti-Gβ blot demonstrated comparable levels of Tγ−Tβ product in the presence and absence of Tα-GDP (panel c, lanes 2 and 4). We concluded that the 43 kDa broad band represents a cross-linked product of POG-Tγ-OMe (8 kDa) and Rh* (35 kDa) because of its reactivity to anti-rhodopsin antibody (data not shown) and the broad shape of the band characteristic of rhodopsin having heteromultimeric carbohydrate chains (*35*). The Tγ−Rh* interaction was eliminated by GTPγS disruption of the Rh*/Tα/Tβγ ternary complex (Figure 3B, panel a, lane 6), indicating a transient interaction between Rh* and the modifying lipid of Tγ in the ternary complex. In order to explore the specificity of this cross-link, Rh*-containing membranes were replaced with opsin membranes, in which rhodopsin was converted to inactive opsin harboring the hydrolyzed chromophore, retinal oxime. In the absence of Tα, the labeling pattern (lanes 7 and 8) was very similar to that observed with Rh*-containing membranes (lanes 1 and 2). In contrast, the 43 kDa broad band was detected far more faintly by anti-Tγ antibody in the membrane fraction (lane 10). This observation supports the conclusion that the Tγ-Rh* cross-link is dependent on the activation state of rhodopsin. The faint broad band of 43 kDa product observed with opsin membranes may represent a very low intrinsic activity of opsin to form the ternary complex capable of activating transducin (*36*). Therefore, the 43 kDa band (lane 10) is probably cross-linked product of Tγ and opsin in the opsin/Tα/Tβγ complex.

In addition to the cross-linked product of Tγ-Rh*, we observed another band showing the anti-Tγ immunoreactivity at the region near the gel front (Figure 3B, panel b, lane 4). This product, which was found only in the membrane but not in the soluble fractions (panel b), exhibited a slightly slower mobility than that of free Tγ and was termed Tγ−X. A faint band of the Tγ−X product was detected in the

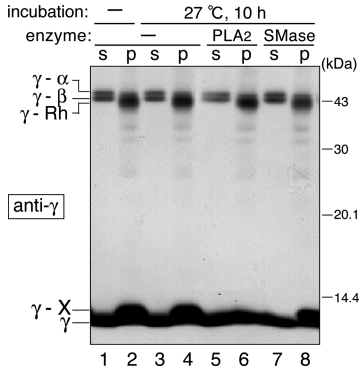

FIGURE 4: Characterization of Tγ−X product. Samples (100 μL, final volume) containing 0.2 μM POG-T$\beta\gamma$-OMe, 0.2 μM Tα, and 1.0 μM Rh* in ROS membranes (at final concentration) were incubated at 4 °C for 30 min and were UV irradiated as described above. After UV irradiation, the samples were centrifuged at 20000*g* at 4 °C for 20 min in order to separate the supernatant from the membrane fraction. These fractions were supplemented with 0.005% (v/v) Triton X-100 and incubated at 27 °C for 10 h in the absence or presence of 10 units of either bee venom phospholipase A_2 (PLA_2, lanes 5 and 6) or *Bacillus* sphingomyelinase (SMase, lanes 7 and 8). Samples were subjected to SDS−PAGE for immunoblot analysis by using anti-Tγ antibody. Shown is a representative set of data from experiments repeated three times with similar results.

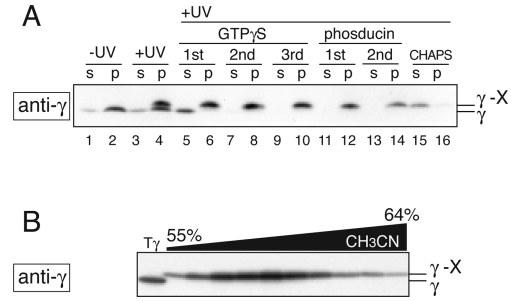

FIGURE 5: Isolation of Tγ−X product from ROS membranes. (A) Immunoblot patterns of the extracted Tγ−X species. The GTPγS-wash and phosducin-extraction procedures were repeated three and two times, respectively. These aliquots of supernatants (s) and pellets (p) were electrophoresed and transferred to a PVDF membrane for immunostaining. Shown is the clipped image of the anti-Tγ blot at the gel front region. (B) Immunoblot patterns of the fractions eluted from the reverse-phase HPLC as described in Experimental Procedures. Each fraction was subjected to SDS−polyacrylamide gel (12.5%) electrophoresis and immunostaining by anti-Tγ antibody. The fractions containing the Tγ−X product (fractions 25−34) are shown.

absence of Tα in the membrane fraction (lane 2), while the band intensity was dramatically increased by the addition of Tα-GDP (lane 4) and markedly reduced by the addition of 10 μM GTPγS (lane 6). This dynamic change of the Tγ−X cross-link level was mostly blunted by replacing Rh*-containing membranes with opsin membranes (lanes 8, 10, and 12). Because the Tγ−X cross-linked product could be degraded by treatment with phospholipase A_2 but not with sphingomyelinase treatment (Figure 4, lanes 6 and 8), the small molecule X was considered as a glycerophospholipid. Collectively, these results demonstrate the transient nature of the Tγ−glycerophospholipid interaction occurring selectively at the stage of the ternary complex formation.

POG Moiety of POG-T$\beta\gamma$-OMe Preferentially Interacts with Phosphatidylethanolamine and Phosphatidylserine. Having obtained evidence for a molecular interaction between Tγ and a lipid species at a specific point in the process of activation of transducin by rhodopsin, we sought to determine whether X, the lipid target of Tγ, represents a specific phospholipid species. To this aim, we performed extraction of Tγ−X product from the membranes. Rh*-containing ROS membranes with POG-T$\beta\gamma$-OMe and Tα were subjected to UV irradiation, and the membranes were then washed with a hypotonic buffer including 10 μM GTPγS to eliminate Tα and POG-T$\beta\gamma$-OMe from the membranes (Figure 5A, lanes 5−10). We then attempted to extract Tγ−X from the washed membranes by adding phosducin, since phosducin is known to extract T$\beta\gamma$ from the membranes by forming a stable soluble complex with T$\beta\gamma$ (*16, 17*). The Tγ−X product was, however, resistant to the phosducin extraction (lanes 11−14). We then solubilized the cross-linked product by using 1.0% CHAPS, after which most of Tγ−X was recovered in the soluble fraction (lanes 15 and 16). The resultant extract (i.e., the soluble fraction) was applied to reverse-phase HPLC equipped with a C4 column and eluted by a linear gradient of CH_3CN. The Tγ−X product was detected in fractions eluted by 55−64% concentration of CH_3CN (Figure 5B) while free POG-Tγ-OMe was eluted in fractions of 47−48% concentration of CH_3CN (not shown). The delayed elution is consistent with X being a hydrophobic lipid.

To trace the identity of X, the purified Tγ−X was subjected to ELISA analysis employing specific lipid-binding probes. We first established the condition in which Tγ−X was adsorbed to the well of the microtiter plate as efficiently as was retinal Tγ when they were probed by anti-Tγ antibody. Under the condition, the wells coated with Tγ−X and retinal Tγ gave comparable signal intensities (Figure 6, panel A). Then we focused our study on PC, PE, PS, SM, and PIP_2, since these lipid species comprise the major population of total phospholipids in bovine ROS membranes (*37*) and PIP_2 level is known to increase in the light (*38*). As shown in Figure 6 (panels B−F), each control lipid was selectively detected by the anti-lipid probes, indicating that these probes recognize their targets in this ELISA analysis. Under the condition, purified Tγ−X showed high reactivities to both anti-PS antibody (panel C) and Ro09-0198 (panel B), a 19 amino acid tetracyclic peptide that specifically binds with PE, whereas the other lipid probes, anti-PC and anti-PIP_2 antibodies and SM-binding peptide lysenin, revealed extremely low signals (panels D−F). In contrast, retinal Tγ showed no reactivities to the two probes, Ro09-0198 or anti-PS antibody (panels B and C). An additional control experiment was performed in this ELISA by immobilizing the lipid background sample derived from the UV-irradiated ROS membranes (ROS control). The wells gave negligible signals toward every probe tested (Figure 6), indicating that the HPLC fraction containing Tγ−X did not contain a significant amount of free lipids that are reactive to the probes. These results indicate that the positive signals observed for the fraction containing Tγ−X toward Ro09-0198 and anti-PS antibody are derived from X. We conclude that the distal tip of the hydrophobic moiety of Tγ C-terminus is located in close vicinity of PE and PS when the Rh*/Tα/T$\beta\gamma$ ternary complex is assembled in the ROS membranes.

DISCUSSION

G protein isoprenylation and carboxyl methylation are indispensable for G protein-regulated signal transduction

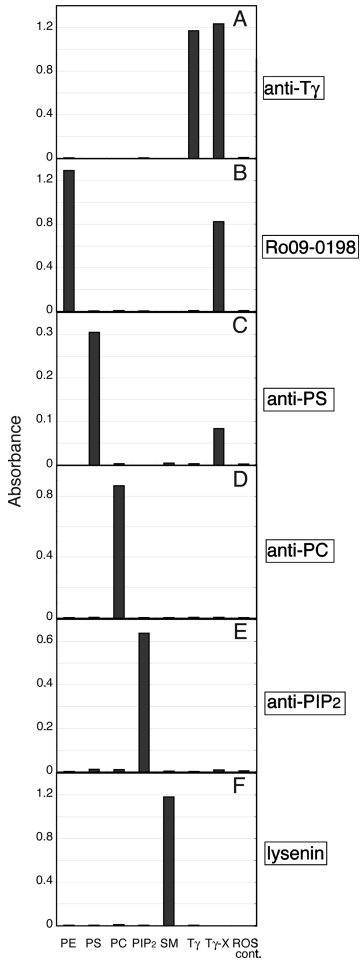

FIGURE 6: Characterization of Tγ−X product by ELISA analysis. Binding of Tγ−X, Tγ, ROS control, and five types of lipids (PE, PS, PC, PIP_2, and SM) was determined by ELISA analysis as described in Experimental Procedures. Sample wells were incubated with (A) anti-Tγ antibody, (B) anti-PE, (C) anti-PS, (D) anti-PC, (E) anti-PIP_2, and (F) anti-SM probes. Abbrevaitions: PE, phosphatidylethanolamine; PS, phosphatidylserine; PC, phosphatidylcholine; PIP_2, phosphatidylinositol 4,5-bisphosphate; SM, sphingomyelin; Tγ−X, the combined pool of fractions in Figure 5B; Tγ, purified farnesyl-Tγ-OMe; ROS-cont., the fraction prepared from the UV-irradiated ROS membrane as described in Experimental Procedures. Shown is a representative set of data from experiments repeated three times with similar results.

processes (*10–13, 21*). These posttranscriptional modifications not only play important roles for the membrane interaction of the modified G proteins but also provide specific protein−protein interaction essential for the G protein signaling. In spite of the importance, the exact sites of the farnesyl group located in the Tα/Tβγ trimer and the Rh*/Tα/Tβγ complex have remained to be determined. In the previous study (*27*), we developed a photoreactive farnesyl analogue POG and demonstrated a dynamic change in molecular interaction of the modifying group depending on the steps in the light signal transduction process. In that study, however, we used a nonmethylated form of POG-Tβγ because it was difficult to obtain a sufficient amount of the methylated form of POG-Tβγ at the time. To circumvent this issue, we have developed an *in vitro* posttranslational modification procedure by enzymatic catalyses with Rce1 and Icmt. To obtain sufficient yields of POG-Tβγ-OMe, we have improved our previous procedures through the following modifications: (i) reduction of the NaCl concentration of the reaction buffer from 150 to 50 mM to prevent association of POG-Tβγ-OMe with the Sf9 cell membranes; (ii) performing the carboxyl methylation reaction at 30 °C to reduce the demethylation reaction. Under the modified conditions employed, we were able to obtain a form of POG-Tβγ-OMe in which the C-terminal cysteine residue was almost completely modified with the methyl group (Figure 1).

Photoaffinity labeling of POG-Tβγ-OMe in the aqueous phase invariably yielded a cross-linked product of Tγ−Tβ (Figure 3A, panels a and c, lane 3), reflecting a constitutive interaction of the C-terminal farnesyl with Tβ. The observed interaction of the modifying group with Tβ is consistent with the previous structural study (*39*), which suggested the presence of the farnesyl-binding pocket in Tβ that is complexed with Tγ and phosducin. The second interaction between the modified group of Tγ and Tα was observed in the aqueous phase, where the Tα/Tβγ heterotrimer formed (Figure 3A, panels a and b, lane 4). These modes of interaction of POG with Tα and Tβ were also observed in the previous study employing the nonmethylated form of POG-Tβγ (*27*). It seems likely that the farnesyl group is invariably located in or close to the propeller structure of Tβ (*39, 40*) and plays an additional role in mediating the subunit−subunit interaction between Tα and Tβ when Tβγ couples with Tα. Consistent with this, a previous report (*13*) demonstrated that the formation of the Tα/Tβγ trimeric complex was disrupted by the synthetic farnesylated peptide corresponding to the C-terminus of Tγ. While structural studies have suggested the N-terminal α-helix of Tα may be the interacting target of the farnesyl group (*22, 23, 39*), our efforts toward identifying the POG-Tγ-linked peptide of Tα resulted in failure due to the low yield of the cross-linked peptide. The relative content of the cross-linked product of Tγ-Tα in total Tα was estimated to be approximately 2% as judged from the distribution of Tα immunoreactivities between free Tα and the Tγ−Tα product (Figure 3A, panel b, lane 4). The low yield is not a reflection of nonspecific interaction because (i) the labeling pattern changed dynamically depending on the signaling state (Figure 3B) and (ii) no labeling was detected for a carrier protein, soybean trypsin inhibitor, that was included in a large excess of POG-Tβγ-OMe in all of the photoaffinity labeling mixtures.

Under conditions in which the Rh*/Tα/Tβγ complex is formed in the ROS membranes, cross-linked products of POG-Tγ-OMe with Rh* and with a low molecular component X were detected in the membrane fraction (Figure 3B, panels a and b, lane 4). The cross-linked product of Tγ−X was degraded by PLA_2, indicating that X is a glycerophospholipid; this third interaction is similar to that we found in our previous study employing the nonmethylated form of POG-Tβγ (*27*). On the other hand, the fourth interaction with Rh* is newly detected in this study, and it was not detectable when we used the nonmethylated form of POG-Tβγ (*27*). It is likely that the interaction of Rh* with Tβγ mediated by the farnesyl group is significantly stabilized by the carboxyl methylation of Tγ. One possible mechanism mediating the stabilization is that the methyl esterification of the C-terminal carboxyl moiety reduces the repulsion between the carboxyl anion and the negatively charged head groups of the membrane phospholipids, which may enable the farnesyl moiety to stick into the lipid bilayer in the close vicinity of Rh*. The results are consistent with our previous observations: The carboxyl methylation of Tγ augments the ability of farnesylated transducin to bind with Rh* (*11*), thereby enhancing the GDP−GTP exchange reaction on Tα catalyzed

by Rh* (*12*). Interestingly, it was shown that a farnesylated (but nonmethylated) oligopeptide mimicking the C-terminal structure of Tγ interacted with Rh* (*41–43*). However, the concentrations of the farnesylated peptide employed in those studies are far greater than that of T$\beta\gamma$ used in the present study. It is likely that the carboxyl methylation of the C-terminus is required for the efficient interaction of Tγ C-terminus with Rh*. Taken together, our data indicate that the modifying group of Tγ interacts with the membrane phospholipid probably as an anchor of Tα-GDP/T$\beta\gamma$ in order for the trimer to couple efficiently with Rh* in the ROS membranes.

In order to identify the molecular species of the phospholipid in the T$\gamma-$X product that was generated at the stage of forming the Rh*/Tα/T$\beta\gamma$ complex (Figure 3B, panel b, lane 4), we extracted the T$\gamma-$X product and performed ELISA analysis using five different types of lipid-binding probes. The T$\gamma-$X product was reactive to Ro09-0198 that is the PE-binding peptide and to anti-PS antibody, but not to anti-PC, anti-PIP_2 antibodies nor lysenin, a SM-binding protein. These data suggest that when the ternary complex is formed, the farnesyl moiety of Tγ interacts preferentially with PE and PS in the ROS membranes. Previous studies showed that PE, PC, PS, PI, and SM make up approximately 38.5−43.0%, 36.0−51.7%, 7.2−13.7%, 1.7−5.9%, and 1.0−3.6%, respectively, of the total phospholipids of the bovine ROS membranes (*37*). The selective interaction between the modifying group of Tγ and PE/PS is explained in several ways. One possibility is that the asymmetric distribution of phospholipids between inner (intradiscal) and outer (cytoplasmic) leaflets of the disk membrane may have caused the preferential labeling of PE/PS. It was reported that the intradiscal leaflet is mainly composed of PC and cholesterol whereas the cytoplasmic leaflet is enriched with PE and PS (*44*). Because the farnesylated T$\beta\gamma$ is predominantly localized at the cytoplasmic surface of the disk membranes, the farnesylated T$\beta\gamma$ may have higher probability to interact with PE and PS rather than with PC, PIP_2, and SM. However, the highly specific pattern of the labeling with PE and PS may not be explained only by this population model. An alternative possibility is that the farnesylated T$\beta\gamma$ might be localized in a membrane microdomain enriched with these particular phospholipids. A considerable number of studies suggests that Rh* in ROS membranes is localized to the distinct membrane domain surrounded by lipids with small head groups such as PE with bulky acyl chains such as docosahexaenoic acid (DHA, 22:6ω3), which together produce a condensed bilayer surface (*45*). In addition, PE with DHA significantly enhances the photochemical activity of rhodopsin (*45*). It is thus possible that the preferential cross-linking observed between the modifying group of Tγ and PE/PS at the stage of forming the Rh*/Tα/T$\beta\gamma$ complex may reflect a unique lipid composition surrounding the complex in the ROS membranes. Hence, in addition to facilitating the coupling of transducin for efficient amplification of the signaling, the farnesylated and methylated C-terminus of Tγ may serve as a sensor to monitor the phospholipid microenvironment of Rh*.

Within our experimental data, it was not possible to identify the target site (atom) in the phospholipid molecule cross-linked with the POG group. In general, active nitrene derived from the azido group preferentially reacts with the electron-rich residue, such as an amino group or a double bond in the acyl chain (*46*). PE and PS have a primary amino group in the polar head and usually retain C=C double bonds in the fatty acid chains. These sites are electron-rich and hence could be good candidates for the cross-linking target with the POG group. When we turn our attention to the position of T$\gamma-$X, we always observed weak signals of T$\gamma-$phospholipid cross-link in the pellet fractions of all the labeling mixtures including those containing inactive opsin in the membranes (Figure 3B, panel b, even numbered lanes). These weak signals might be partly attributable to the inherent chemical reactivity of the phospholipids such as PE and PS having the amino group in the polar head. On the other hand, in the presence of light-activated rhodopsin and transducin trimers (Figure 3B, panel b, lane 4), the T$\gamma-$phospholipid cross-linked product gave a selectively strong signal, and this product was extracted and analyzed in detail (Figures 5 and 6). Here we should emphasize that, in the ELISA analysis, the T$\gamma-$X was detected by cyclic antibiotic peptide Ro09-0198 and anti-PS antibody that recognize strictly the structure of PE and PS, respectively. In particular, the PE head group including the primary amine at the ethanolamine moiety is indispensable for the recognition of PE by Ro09-0198, and chemical modifications of the primary amine abolish completely the recognition (*47*). It is thus likely that the distal tip of the farnesyl analogue is predominantly cross-linked with the acyl chains rather than the head group of PE and PS. When applied to the farnesyl, the distal end would stick deep into the membrane bilayer as an anchor or as an interface between Rh* and the surrounding phospholipids when the Rh*/Tα/T$\beta\gamma$ ternary complex is assembled. Importantly, the degree of this interaction with the phospholipids is not static but highly variable depending on the receptor activation (Figure 3B, panel b). The weak signals of T$\gamma-$X cross-link constantly observed in the membrane fraction under various conditions (Figure 3B, panel b) are suggestive of location of the modifying lipid of Tγ in equilibrium between the Tβ pocket and the lipid layer surface, when the receptor is in the resting state of signaling.

In summary, we have developed a novel analogue of fully modified T$\beta\gamma$ for photoaffinity labeling studies and demonstrated that the modifying group of Tγ mediates both the protein−protein and the protein−membrane interactions in Rh*/Tα/T$\beta\gamma$ complex formation. The farnesyl-Rh* or farnesyl-PE/PS interaction appears to facilitate transducin to form efficiently the ternary complex with Rh*. Further analysis of the cross-linked lipids may provide insight into the mechanism underlying the dynamic formation of the Rh*/Tα/T$\beta\gamma$ complex in the ROS membranes.

ACKNOWLEDGMENT

We thank Dr. Yoshikazu Ohya (The University of Tokyo) for the kind gift of FTase expression vector.

REFERENCES

1. Arshavsky, V. Y., Lamb, T. D., and Pugh, E. N., Jr. (2002) G proteins and phototransduction. *Annu. Rev. Physiol. 64*, 153–187.
2. Fukada, Y., Takao, T., Ohguro, H., Yoshizawa, T., Akino, T., and Shimonishi, Y. (1990) Farnesylated γ-subunit of photoreceptor G protein indispensable for GTP-binding. *Nature 346*, 658–660.
3. Lai, R. K., Perez-Sala, D., Canada, F. J., and Rando, R. R. (1990) The γ subunit of transducin is farnesylated. *Proc. Natl. Acad. Sci. U.S.A. 87*, 7673–7677.

4. Matsuda, T., and Fukada, Y. (2000) Functional analysis of farnesylation and methylation of transducin. *Methods Enzymol. 316*, 465–481.
5. Casey, P. J., and Seabra, M. C. (1996) Protein prenyltransferases. *J. Biol. Chem. 271*, 5289–5292.
6. Otto, J. C., Kim, E., Young, S. G., and Casey, P. J. (1999) Cloning and characterization of a mammalian prenyl protein-specific protease. *J. Biol. Chem. 274*, 8379–8382.
7. Hrycyna, C. A., Sapperstein, S. K., Clarke, S., and Michaelis, S. (1991) The *Saccharomyces cerevisiae* STE14 gene encodes a methyltransferase that mediates C-terminal methylation of α-factor and RAS proteins. *EMBO J. 10*, 1699–1709.
8. Bergo, M. O., Leung, G. K., Ambroziak, P., Otto, J. C., Casey, P. J., and Young, S. G. (2000) Targeted inactivation of the isoprenylcysteine carboxyl methyltransferase gene causes mislocalization of K-Ras in mammalian cells. *J. Biol. Chem. 275*, 17605–17610.
9. Simonds, W. F., Butrynski, J. E., Gautam, N., Unson, C. G., and Spiegel, A. M. (1991) G-protein beta gamma dimers. Membrane targeting requires subunit coexpression and intact gamma C-A-A-X domain. *J. Biol. Chem. 226*, 5363–5366.
10. Hancock, J. F., Cadwallader, K., and Marshall, C. J. (1991) Methylation and proteolysis are essential for efficient membrane binding of prenylated p21K-ras(B). *EMBO J. 10*, 641–646.
11. Ohguro, H., Fukada, Y., Takao, T., Shimonishi, Y., Yoshizawa, T., and Akino, T. (1991) Carboxyl methylation and farnesylation of transducin γ-subunit synergistically enhance its coupling with metarhodopsin II. *EMBO J. 10*, 3669–3674.
12. Fukada, Y., Matsuda, T., Kokame, K., Takao, T., Shimonishi, Y., Akino, T., and Yoshizawa, T. (1994) Effects of carboxyl methylation of photoreceptor G protein γ-subunit in visual transduction. *J. Biol. Chem. 269*, 5163–5170.
13. Matsuda, T., Takao, T., Shimonishi, Y., Murata, M., Asano, T., Yoshizawa, T., and Fukada, Y. (1994) Characterization of interactions between transducin α/βγ-subunits and lipid membranes. *J. Biol. Chem. 269*, 30358–30363.
14. Hancock, J. F., Magee, A. I., Childs, J. E., and Marshall, C. J. (1989) All ras proteins are polyisoprenylated but only some are palmitoylated. *Cell 57*, 1167–1177.
15. Inglese, J., Koch, W. J., Caron, M. G., and Lefkowitz, R. J. (1992) Isoprenylation in regulation of signal transduction by G-protein-coupled receptor kinases. *Nature 359*, 147–150.
16. Lee, R. H., Lieberman, B. S., and Lolley, R. N. (1987) A novel complex from bovine visual cells of a 33,000-dalton phosphoprotein with β- and γ-transducin: purification and subunit structure. *Biochemistry 26*, 3983–3990.
17. Lee, B. Y., Thulin, C. D., and Willardson, B. M. (2004) Site-specific phosphorylation of phosducin in intact retina. Dynamics of phosphorylation and effects on G protein βγ dimer binding. *J. Biol. Chem. 279*, 54008–54017.
18. Sokolov, M., Strissel, K. J., Leskov, I. B., Michaud, N. A., Govardovskii, V. I., and Arshavsky, V. Y. (2004) Phosducin facilitates light-driven transducin translocation in rod photoreceptors. Evidence from the phosducin knockout mouse. *J. Biol. Chem. 279*, 19149–19156.
19. Rosenzweig, D. H., Nair, K. S., Wei, J., Wang, Q., Garwin, G., Saari, J. C., Chen, C. K., Smrcka, A. V., Swaroop, A., and Lem, J. (2007) Subunit dissociation and diffusion determine the subcellular localization of rod and cone transducins. *J. Neurosci. 27*, 5484–5494.
20. Higgins, J. B., and Casey, P. J. (1994) In vitro processing of recombinant G protein γ subunits. Requirements for assembly of an active βγ complex. *J. Biol. Chem. 269*, 9067–9073.
21. Parish, C. A., Smrcka, A. V., and Rando, R. R. (1995) Functional significance of beta gamma-subunit carboxymethylation for the activation of phospholipase C and phosphoinositide 3-kinase. *Biochemistry 34*, 7722–7727.
22. Wall, M. A., Coleman, D. E., Lee, E., Iniguez-Lluhi, J. A., Posner, B. A., Gilman, A. G., and Sprang, S. R. (1995) The structure of the G protein heterotrimer Gi α_1 β_1 γ_2. *Cell 83*, 1047–1058.
23. Lambright, D. G., Sondek, J., Bohm, A., Skiba, N. P., Hamm, H. E., and Sigler, P. B. (1996) The 2.0 Å crystal structure of a heterotrimeric G protein. *Nature 379*, 311–319.
24. Edelstein, R. L., and Distefano, M. D. (1997) Photoaffinity labeling of yeast farnesyl protein transferase and enzymatic synthesis of a Ras protein incorporating a photoactive isoprenoid. *Biochem. Biophys. Res. Commun. 235*, 377–382.
25. Bukhtiyarov, Y. E., Omer, C. A., and Allen, C. M. (1995) Photoreactive analogues of prenyl diphosphates as inhibitors and probes of human protein farnesyltransferase and geranylgeranyltransferase type I. *J. Biol. Chem. 270*, 19035–19040.
26. Quellhorst, G. J., Jr., Allen, C. M., and Wessling-Resnick, M. (2001) Modification of Rab5 with a photoactivatable analog of geranylgeranyl diphosphate. *J. Biol. Chem. 276*, 40727–40733.
27. Hagiwara, K., Wada, A., Katadae, M., Ito, M., Ohya, Y., Casey, P. J., and Fukada, Y. (2004) Analysis of the molecular interaction of the farnesyl moiety of transducin through the use of a photoreactive farnesyl analogue. *Biochemistry 43*, 300–309.
28. Nam, K. S., Igarashi, K., Umeda, M., and Inoue, K. (1990) Production and characterization of monoclonal antibodies that specifically bind to phosphatidylcholine. *Biochim. Biophys. Acta 1046*, 89–96.
29. Miyazawa, A., Umeda, M., Horikoshi, T., Yanagisawa, K., Yoshioka, T., and Inoue, K. (1988) Production and characterization of monoclonal antibodies that bind to phosphatidylinositol 4,5-bisphosphate. *Mol. Immunol. 25*, 1025–1031.
30. Yamaji, A., Sekizawa, Y., Emoto, K., Sakuraba, H., Inoue, K., Kobayashi, H., and Umeda, M. (1998) Lysenin, a novel sphingomyelin-specific binding protein. *J. Biol. Chem. 273*, 5300–5306.
31. Choung, S. Y., Kobayashi, T., Inoue, J., Takemoto, K., Ishitsuka, H., and Inoue, K. (1988) Hemolytic activity of a cyclic peptide Ro09-0198 isolated from Streptoverticillium. *Biochim. Biophys. Acta 940*, 171–179.
32. Chen, W. J., Moomaw, J. F., Overton, L., Kost, T. A., and Casey, P. J. (1993) High level expression of mammalian protein farnesyltransferase in a baculovirus system. The purified protein contains zinc. *J. Biol. Chem. 268*, 9675–9680.
33. De Busser, H. M., Van Dessel, G. A., and Lagrou, A. R. (2000) Identification of prenylcysteine carboxymethyltransferase in bovine adrenal chromaffin cells. *Int. J. Biochem. Cell Biol. 32*, 1007–1016.
34. Laemmli, U. K. (1970) Cleavage of structural proteins during the assembly of the head of bacteriophage T4. *Nature 227*, 680–685.
35. Kaushal, S., Ridge, K. D., and Khorana, H. G. (1994) Structure and function in rhodopsin: the role of asparagine-linked glycosylation. *Proc. Natl. Acad. Sci. U.S.A. 91*, 4024–4028.
36. Melia, T. J., Jr., Cowan, C. W., Angleson, J. K., and Wensel, T. G. (1997) A comparison of the efficiency of G protein activation by ligand-free and light-activated forms of rhodopsin. *Biophys. J. 73*, 3182–3191.
37. Daeman, F. J. (1973) Vertebrate rod outer segment membranes. *Biochim. Biophys. Acta 300*, 255–288.
38. Grigorjev, I. V., Grits, A. I., Artamonov, I. D., Baranova, L. A., and Volotovski, I. D. (1996) betagamma-Transducin stimulates hydrolysis and synthesis of phosphatidylinositol 4,5-bisphosphate in bovine rod outer segment membranes. *Biochim. Biophys. Acta 1310*, 131–136.
39. Loew, A., Ho, Y. K., Blundell, T., and Bax, B. (1998) Phosducin induces a structural change in transducin beta gamma. *Structure 6*, 1007–1019.
40. Myung, C. S., and Garrison, J. C. (2000) Role of C-terminal domains of the G protein beta subunit in the activation of effectors. *Proc. Natl. Acad. Sci. U.S.A. 97*, 9311–9316.
41. Kisselev, O., Ermolaeva, M., and Gautam, N. (1995) Efficient interaction with a receptor requires a specific type of prenyl group on the G protein γ subunit. *J. Biol. Chem. 270*, 25356–25358.
42. McCarthy, N. E., and Akhtar, M. (2000) Function of the farnesyl moiety in visual signalling. *Biochem. J. 347*, 163–171.
43. Bartl, F., Ritter, E., and Hofmann, K. P. (2000) FTIR spectroscopy of complexes formed between metarhodopsin II and C-terminal peptides from the G-protein α- and γ-subunits. *FEBS Lett. 473*, 259–264.
44. Wu, G., and Hubbell, W. L. (1993) Phospholipid asymmetry and transmembrane diffusion in photoreceptor disc membranes. *Biochemistry 32*, 879–888.
45. Brown, M. F. (1994) Modulation of rhodopsin function by properties of the membrane bilayer. *Chem. Phys. Lipids 73*, 159–180.
46. Bayley, H., and Knowles, J. R. (1977) Photoaffinity labeling. *Methods Enzymol. 46*, 69–114.
47. Emoto, K., Kobayashi, T., Yamaji, A., Aizawa, H., Yahara, I., Inoue, K., and Umeda, M. (1996) Redistribution of phosphatidylethanolamine at the cleavage furrow of dividing cells during cytokinesis. *Proc. Natl. Acad. Sci. U.S.A. 93*, 12867–12872.

BI800359H